Keratinocytes produce IL-17c to protect peripheral nervous systems during human HSV-2 reactivation

Tao Peng,[1,4] R. Savanh Chanthaphavong,[1]* Sijie Sun,[1]* James A. Trigilio,[1] Khamsone Phasouk,[4] Lei Jin,[4] Erik D. Layton,[4] Alvason Z. Li,[4] Colin E. Correnti,[5] Willem De van der Schueren,[5] Julio Vazquez,[6] Diana R. O'Day,[3] Ian A. Glass,[3] David M. Knipe,[7] Anna Wald,[1,2,4] Lawrence Corey,[1,2,4] and Jia Zhu[1,4]

[1]Department of Laboratory Medicine, [2]Department of Medicine, and [3]Laboratory of Developmental Biology, University of Washington, Seattle, WA
[4]Vaccine and Infectious Disease Division, [5]Clinical Research Division, and [6]Shared Resources Scientific Imaging, Fred Hutchinson Cancer Research Center, Seattle, WA
[7]Department of Microbiology and Immunobiology, Harvard Medical School, Boston, MA

Despite frequent herpes simplex virus (HSV) reactivation, peripheral nerve destruction and sensory anesthesia are rare. We discovered that skin biopsies obtained during asymptomatic human HSV-2 reactivation exhibit a higher density of nerve fibers relative to biopsies during virological and clinical quiescence. We evaluated the effects of HSV infection on keratinocytes, the initial target of HSV replication, to better understand this observation. Keratinocytes produced IL-17c during HSV-2 reactivation, and IL-17RE, an IL-17c–specific receptor, was expressed on nerve fibers in human skin and sensory neurons in dorsal root ganglia. In ex vivo experiments, exogenous human IL-17c provided directional guidance and promoted neurite growth and branching in microfluidic devices. Exogenous murine IL-17c pretreatment reduced apoptosis in HSV-2–infected primary neurons. These results suggest that IL-17c is a neurotrophic cytokine that protects peripheral nerve systems during HSV reactivation. This mechanism could explain the lack of nerve damage from recurrent HSV infection and may provide insight to understanding and treating sensory peripheral neuropathies.

The Journal of Experimental Medicine

INTRODUCTION

Keratinocytes, immune cells, and nerve fibers are interconnected anatomically and functionally in skin (Misery, 1997; Chuong et al., 2002). HSV types 1 and 2 (HSV-1 and HSV-2) have evolved strategies to exploit this system for recurrent infection. After primary infection at the site of acquisition (mouth and genitals), viruses travel retrogradely via axons to cell bodies of peripheral sensory neurons, where they establish latency. Reactivation from latency involves anterograde movement to sites near the original site of entry for replication and transmission (Roizman and Whitley, 2013). Human recurrent HSV-2 infection is frequent and often clinically asymptomatic (Wald et al., 1997; Johnston et al., 2012; Schiffer et al., 2013). Although sensory anesthesia may precede or accompany HSV-2 reactivation, reports of such peripheral nerve damage or neuropathy are extremely rare among patients with HSV-2 recurrent infection, a clinical observation that distinguishes it markedly from varicella zoster virus infection, in which nerve destruction and neuropathy are well recognized (Schmader, 1998; Haanpää et al., 1999). It is unclear how peripheral nerves maintain their function in spite of frequent HSV-2 reactivation over time. In fact, there is controversy whether peripheral nerve damage is associated with human HSV-2 reactivation.

The IL-17 family consists of six members (IL-17a, IL-17b, IL-17c, IL-17d, IL-17e, and IL-17f; Gaffen, 2009, 2011). To date IL-17c has been identified as an epithelial cell–derived cytokine that regulates innate immune function (Ramirez-Carrozzi et al., 2011; Song et al., 2011) and promotes inflammation in psoriasis (Ramirez-Carrozzi et al., 2011; Johnston et al., 2013). Here we report that both keratinocytes and neurons produce IL-17c in response to HSV-2 infection and that IL-17c functions as a neurotrophic factor that provides a survival signal to protect sensory neurons from apoptosis during HSV infection and, most importantly, stimulates peripheral nerve growth.

RESULTS

Interaction of keratinocytes and nerve fibers via IL-17c/IL-17RE during human recurrent HSV-2 infection

Previously, we showed spatial close proximity among cutaneous nerve endings, basal keratinocytes, and CD8$^+$ T cells in biopsy tissues taken during HSV-2 asymptomatic reacti-

*R.S. Chanthaphavong and S. Sun contributed equally to this paper.

Correspondence to Tao Peng: tpeng@uw.edu; Jia Zhu: jiazhu@uw.edu

Abbreviations used: BDNF, brain-derived neurotrophic factor; DRG, dorsal root ganglia; HSN, human sensory neuron; LCM, laser capture microdissection; MCN, mouse primary cortical neuron; mIL-17c, murine IL-17c; MOI, multiplicity of infection; NCAM, neural cell adhesion molecule; NGF, nerve growth factor; ODN, oligodeoxynucleotide; PGN, peptidoglycan.

The Rockefeller University Press
J. Exp. Med. 2017 Vol. 214 No. 8 2315–2329
https://doi.org/10.1084/jem.20160581

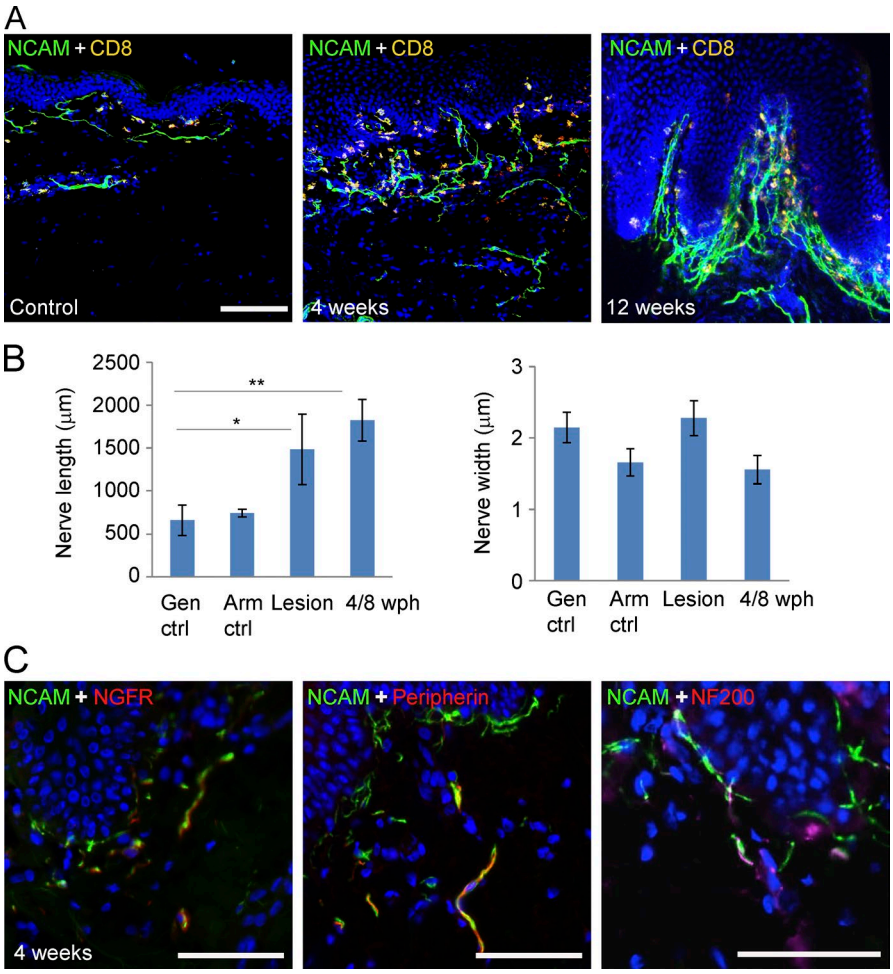

Figure 1. **Nerve fiber growth during HSV-2 reactivation.** (A) Nerve fibers in skin biopsies at time of subclinical HSV-2 reactivation (shedding) are stained for NCAM (green). An increased number of NCAM$^+$ nerve fibers in the area just below the dermal epidermal junction, the site of HSV-2 reactivation, is seen as compared with control biopsy obtained from contralateral genital skin. Cells were costained with an anti-CD8a antibody (yellow) and DAPI (blue). Bar, 100 µm. (B) Comparison of length and width of NCAM$^+$ nerve fibers among biopsies obtained at time of HSV-2 lesion (Lesion), 4 and 8 wk posthealed (4/8 wph), contralateral control biopsies (Gen ctrl), and arm control biopsies (Arm ctrl; n = 10). *, P = 0.043; **, P = 0.031. P-values are derived from paired two-sample t tests. (C) NCAM$^+$ nerve fibers express NGFR and intermediate filaments (peripherin and NF200). Tissue of 4 wk posthealed asymptomatic shedding skin biopsies was double stained with anti-NCAM (green) and NGFR (red), peripherin (red) or NF200 (red) antibodies. Bar, 50 µm.

vation (Zhu et al., 2007, 2009, 2013). To explore the impact of recurrent HSV-2 infection on peripheral nerves, we first measured the length and width of neural cell adhesion molecule (NCAM)$^+$ nerve fibers in genital skin biopsies taken at the time of symptomatic and asymptomatic reactivation and compared them with control genital skin biopsies in contralateral sites taken from areas without HSV reactivation. Peripheral nerve fibers in tissues undergoing HSV asymptomatic shedding had a much higher density compared with nerve fibers detected in control skin (Fig. 1 A). Nerve fibers in posthealed skin biopsies showing recent HSV-2 reactivation were much longer on average compared with those in matching contralateral controls (P = 0.031, n = 10), while the width of nerve fibers was similar (Fig. 1 B). Nerve fibers in lesion biopsies also exhibited the increased length relative to those of controls (P = 0.043, n = 10). The HSV-2 DNA copy numbers in biopsies from the 10 patients are provided in Table S1. NCAM$^+$ nerve fibers in posthealed skin biopsies also coexpressed the low-affinity nerve growth factor receptor. Both peripherin$^+$ and NF200$^+$ nerve fibers were present in posthealed skin biopsies (Fig. 1 C). These results suggest that neurotrophins might be released locally to stimulate nerve growth and/or repair nerve endings in response to HSV-2 reactivation.

To evaluate the role(s) of keratinocytes in influencing nerve fiber density during recurrent HSV-2 infection, we selectively recovered individual basal keratinocytes by laser capture microdissection (LCM) from human genital skin biopsies at the time of acute lesion and asymptomatic shedding subsequently at 4 or 8 wk posthealing as well as contralateral control biopsies from the same patients (n = 4) and compared their transcriptional profiles (Fig. 2 A). Expression of keratin 5 and 14, markers of basal keratinocytes in the human epidermis (Lloyd et al., 1995), was measured in isolated keratinocytes as well as CD1a$^+$ Langerhans cells and CD8a$^+$ T cells (Fig. 2 B; Peng et al., 2012; Zhu et al., 2013). The isolated keratinocytes expressed ~10 times higher levels of keratin 5 and 14 than the other cell types yet expressed much less CD1a and CD8a compared with captured CD1a$^+$ and CD8a$^+$ cells, respectively, suggesting a pure cell population. Illumina Human HT-12 bead arrays contain ~300 genes annotated as growth factor/cytokine/chemokine activity; 3 were significantly induced in keratinocytes isolated from HSV-2 lesion and posthealed biopsies (IL-17c, CCL5, and TNFSF10), and 6 were

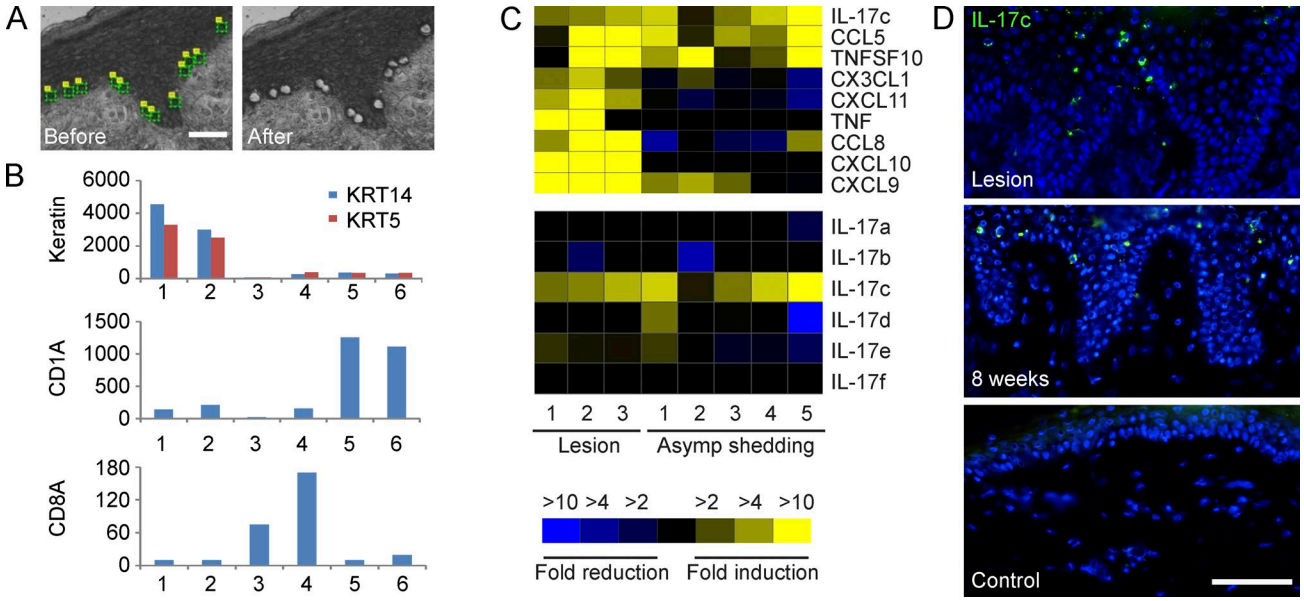

Figure 2. **Recurrent HSV-2 infection induces IL-17c expression in keratinocytes.** (A) Isolation of keratinocytes above basement membrane by LCM. (B) Expression of keratin 5 (KRT5) and 14 (KRT14), CD1a and CD8a in laser-captured keratinocytes (kera), $CD1a^+$ Langerhans cells (LC), and $CD8a^+$ CD8 T cells (CD8) from control (ctrl) and posthealed (PH) genital skin biopsies during recurrent HSV-2 infection. Y-axis, intensity values from normalized Illumina bead array data. The displayed values are the means for keratinocytes ($n = 4$), $CD1a^+$ Langerhans cells ($n = 8$), and $CD8a^+$ CD8 T cells ($n = 8$). 1, kera_ctrl; 2, kera_PH; 3, CD8_ctrl; 4, CD8_PH; 5, LC_ctrl; and 6, LC_PH. (C) HSV infection in keratinocytes induced IL-17c expression in vivo. Comparison of expression of cytokines/chemokines (top) and six different members of IL-17 (bottom) in keratinocytes isolated from lesion and posthealed skin (asymptomatic shedding) biopsies to those from contralateral control biopsies. (D) IL-17c protein expression in epidermal keratinocytes in skin biopsies during lesion and shedding (clinical quiescence 8-wk shedding). IL-17c expression was detected by immunofluorescent staining with an anti-IL-17c antibody (green) and nuclei stained with DAPI (blue). Bar, 50 µm.

up-regulated only in keratinocytes from lesions (CX3CL1, CXCL11, TNF, CCL8, CXCL10, and CXCL9; Fig. 2 C, top). Among the six related IL-17 family members, IL-17c, a predominantly epithelial-derived cytokine (Gaffen, 2009; Ramirez-Carrozzi et al., 2011; Song et al., 2011), was the only induced gene in keratinocytes during recurrent HSV-2 infection (Fig. 2 C, bottom). Immunofluorescent staining indicated that IL-17c was expressed in small populations of keratinocytes exclusively in the epidermis in lesion and posthealed skin biopsies but not in control biopsies (Fig. 2 D).

To test the hypothesis that HSV-2 reactivation could induce IL-17c in keratinocytes, we cultured human primary keratinocytes and evaluated whether these cells would in vitro produce IL-17c in response to HSV-2 infection over 12 h. Peak induction occurred at 6 h postinfection (hpi) and remained at elevated levels when infected with UV-inactivated virus or acyclovir treatment (Fig. 3 A, left). Virus titer assays suggest that virus (HSV-2) titers barely changed during the first 6 hpi, yet virus titers increased 100-fold between 6 and 24 hpi; in contrast, virus titers during infection with UV-inactivated HSV-2 or HSV-2 in the presence of acyclovir were consistently low during the entire time course (Fig. 3 A, middle). HSV-1 (KOS strain) also induced IL-17c expression in a similar kinetic with peak induction around 5 hpi (Fig. 3 A, right). An HSV-1 mutant with deletion in ICP0, an immediate early gene, eliminated the IL-17c production during the time course of infection (not depicted). Collectively, the data suggest that early infection induced IL-17c expression in keratinocytes but HSV infection at a late stage reduced its expression. Furthermore, immunofluorescent staining demonstrated IL-17c expression at the cell surface and in the cytoplasm in cultured keratinocytes infected with the HSV-2 strain HG-52 (Fig. 3 B). Relative to mock infection, HG-52 infection at a multiplicity of infection (MOI) of 1 and 10 induced 1.7- and 7.6-fold increase in the number of $IL\text{-}17c^+$ cells at 7 hpi, respectively (Fig. 3 B). Thus, HSV-2 infection induces IL17c expression in human primary keratinocytes.

As peptidoglycan (PGN) and flagellin, bacterial ligands for TLR2 and TLR5, respectively, have been shown to stimulate IL-17c expression in keratinocytes (Ramirez-Carrozzi et al., 2011), we evaluated whether TLR signaling mediates HSV infection–induced IL-17c expression. HSV infection has been shown to induce host innate immune responses through pattern recognition receptors such as TLRs and RIG-I like receptors (Lund et al., 2003; Kurt-Jones et al., 2004; Sato et al., 2006; Rasmussen et al., 2009; Reinert et al., 2012; Svensson et al., 2012). Flagellin, a bacterial TLR5 ligand, potently induced IL-17c expression at 6 and 24 h posttreatment; in contrast, poly(I:C)/LyoVec (a RIG-I ligand)

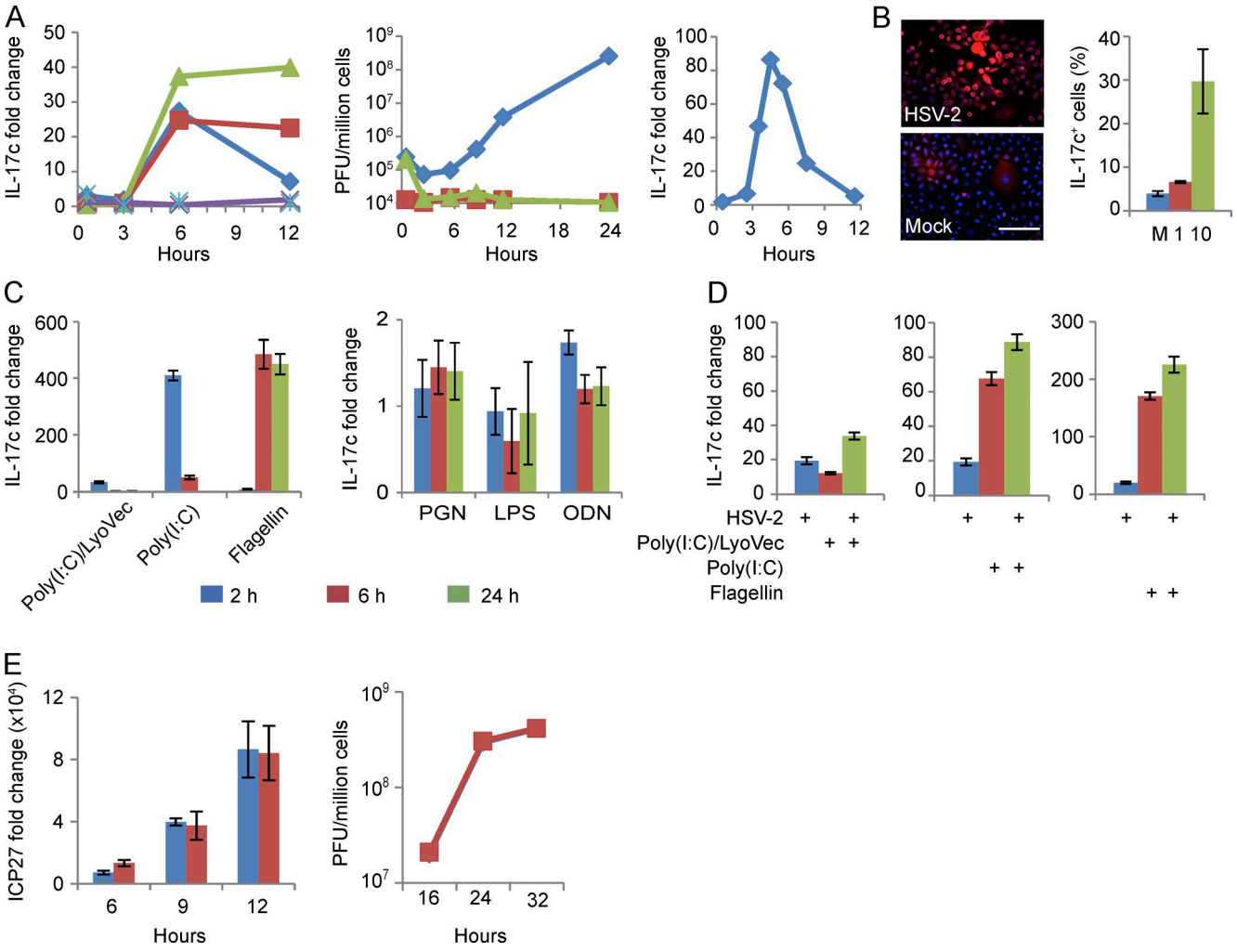

Figure 3. **HSV-2 infection in human primary keratinocytes induces IL-17c, which does not appear to have significant antiviral effect.** (A) IL-17c expression in HSV infected human primary keratinocytes. IL-17c RNA expression in a time course of HSV-2-infected keratinocytes (left). Cells were mock infected (aqua) or infected with HSV-2 (HG52; MOI = 1) in the absence (blue) or presence (green) of acyclovir (30 µM) or with UV-inactivated viruses (red). Purple is acyclovir without virus. Y-axis is fold change of RNA levels above mock infected cells; x-axis is time after infection in hours. HSV-2 virus growth curve in primary keratinocytes was determined by plaque assay (middle). Y-axis is PFU (plaque forming units) per million cells; x-axis is time post-infection (hours) of HSV-2 in the absence (blue) or presence (green) of acyclovir or UV-inactivated viruses (red). IL-17c expression in a time course of HSV-1-infected human primary keratinocytes (right). Cells were mock infected or infected with HSV-1 (KOS; MOI of 1). (B) IL-17c protein expression in HSV-2-infected keratinocytes. Cells mock (bottom) or HSV-2 infected (top) for 7 h at MOIs of 1 and 10 were analyzed for IL-17c expression by immunofluorescent staining with an anti–IL-17c antibody (red). Nuclei stained with DAPI (blue). Graph is quantification of staining as the percentage of IL-17c-expressing cells. M, mock; 1, MOI of 1; 10, MOI of 10. Bar, 50 µm. (C and D) HSV-2 and TLR ligands additively induced IL-17c expression in human primary keratinocytes. Cells were treated with TLR ligands (PGN, poly[I:C]/LyoVec, poly[I:C], LPS, flagellin, and ODN) for 2, 6, and 24 h (C) or infected with HSV-2 for 3 h and then treated with poly[I:C]/LyoVec, poly[I:C], or flagellin for another 4 h (D). Y-axis, IL-17c RNA expression fold changes relative to untreated and mock infected controls. (E) Blocking IL-17c signaling does not have significant effect on HSV-2 gene expression or viral titers in infected human primary keratinocytes. Cells were pretreated with an IL-17RA neutralizing antibody (red) or matching control IgG (blue) for 1 h before HSV-2 infection. Gene expression (*ICP27*) was assayed by quantitative PCR (left), and viral titers were determined by plaque assay in Vero cells (right). Error bars represent 1 standard deviation from the mean of three replicates. All the experiments were repeated three times.

and poly(I:C) (a TLR3 ligand) induced the highest IL-17c expression at 2 h. PGN (a TLR2 ligand) and oligodeoxynucleotide (ODN; a TLR9 ligand) induced only a small increase and LPS (a TLR4 ligand) had no effect on IL-17c expression (Fig. 3 C). The combination of HSV-2 infection (7 h) and flagellin, poly(I:C)/LyoVec, or Poly(I:C) treatment (4 h) additively induced IL-17c expression (Fig. 3 D). These findings suggest that HSV infection and flagellin, poly(I:C)/LyoVec, or Poly(I:C) independently induce IL-17c expression in cultured human primary keratinocytes.

To understand biological functions of HSV-2-induced IL-17c in keratinocytes, we first examined its potential antiviral activity. Blocking IL-17c signaling using a neutralizing antibody for IL-17RA, a receptor subunit for IL-17c, did not influence HSV gene expression (*ICP27*) or HSV titers in human primary keratinocytes (Fig. 3 E). This lack of antiviral activity in vitro led us to explore potential target cells of IL-17c during HSV-2 reactivation in vivo. We first performed immunofluorescent staining of IL-17RE, the receptor subunit specific for IL-17c (Chang et al., 2011; Ramirez-Carrozzi et al., 2011; Song et al., 2011). IL-17RE expression was not found on $CD15^+$, $CD8^+$, or $CD4^+$ immune cells, markers of neutrophils and T cells, respectively, but was found on structures with elongated fiber like shapes and in keratinocytes (Fig. 4 A, left). Dual staining for IL-17RE and NCAM or peripherin showed that IL-17RE was detected on $NCAM^+$ and $peripherin^+$ nerve fibers in skin biopsies during active and asymptomatic HSV-2 infection as well as in control biopsies (Fig. 4 A, right; and Fig. 4, B and C, left). We also detected IL-17RA expression in control and posthealed skin biopsies (Fig. 4, B and C, right). These data suggest that neuronal cells may be the targets of keratinocyte-produced IL-17c.

To further investigate the neuronal expression of IL-17RE, we examined dorsal root ganglia (DRG) from human fetal tissue. The expression of IL-17RE protein was detected in both soma and axonal regions of DRG (Fig. 4 D). Dual in situ hybridization confirmed IL-17RE mRNA expression in β-tubulin III^+ neurons and also in β-tubulin III^- cells (Fig. 4 E). IL-17RE was expressed in a subset of $NF200^+$ or $peripherin^+$ sensory neurons (Fig. 4 F), consistent with its expression patterns observed in the genital skin (Fig. 4, A–C). These findings indicate an abundance of IL-17RE in the peripheral nerve system and provide circumstantial evidence that IL-17c released from epidermal keratinocytes could interact with IL-17RE on nerve fibers in the dermal area during the process of HSV-2 reactivation.

IL-17c induces neurite growth of human neuroblastoma cells and primary sensory neurons

To determine if IL-17c might be related to the peripheral neurite growth seen in skin biopsies, we conducted a series of studies evaluating if exogenous recombinant IL-17c could induce neurite growth. Using a two-chamber microfluidic device, we noticed that differentiated SY5Y neuron-like cells (Abemayor and Sidell, 1989) exhibited visible neurites extending into microgroove channels after 24 h in the IL-17c–containing device. During the next 10 d, significantly more and longer neurites grew into the main channel with basal medium plus IL-17c compared with medium only (Fig. 5, A and B). We demonstrated nerve growth factor (NGF) and brain-derived neurotrophic factor (BDNF), two known neurotrophic factors, also induced such effects. The neurotrophic effects of IL-17c, NGF, or BDNF were significantly inhibited by neutralizing antibodies for IL-17RA, NGF, or BDNF, respectively (Fig. 5, A and B). Furthermore, we have purified human and murine IL-17c, human IL-17RA and IL-17RE protein expressed in an in-house mammalian expression system (see detailed information in Materials and methods and Fig. S1). Size-exclusion shift assays uncovered that IL-17c forms a ternary complex with IL-17RA and IL-17RE as well as a binary complex with IL-17RE (Fig. 5 C), which is consistent with the literature showing that IL-17RA and IL-17RE form a heterodimer to interact with IL-17c (Ramirez-Carrozzi et al., 2011; Song et al., 2011). Collectively, the data suggest that IL-17c can stimulate neurite growth of cultured human neuroblastoma cells.

We next isolated human sensory neurons (HSNs) from fetal DRG. HSNs were cultured in full neural medium or such medium with IL-17c or NGF for 3 d before the cells were live-imaged to measure neurite length, branch points, and cell body area hourly for 16 h (Fig. 6 A). Neurites grew longer and faster with more branches in the presence of IL-17c compared with culture medium alone or medium plus NGF. In contrast, the growth rates of cell body were similar in all three conditions during the 16-–h time period (Fig. 6, B and C). To measure the effect of IL-17c on directional neurite growth, we used a three-chamber microfluidic device in which HSNs were placed in the middle channel, and the left and right channels contained full medium and full medium plus IL-17c, respectively (Fig. 6 D). By day 10, significantly more neurites grew into the IL-17c-containing channel than into the medium-alone channel. On day 16, cells were fixed and stained with PGP9.5 and IL-17RE antibodies. Compared with those in the channel with medium alone, almost twice as many neurites were found in the IL-17c containing channel, with 2.7-fold longer total neurites and 3.5-fold more branch points (Fig. 6, E and F). Neurites in the IL-17c channel were $IL\text{-}17RE^+$ and appeared to have larger growth cones compared with those in the medium-alone channel (Fig. 6, G and H). Collectively, the data suggest that IL-17c appears to be a neurotrophic factor promoting neurite growth and branching for HSNs.

Pretreatment with IL-17c reduces apoptosis during HSV infection of murine primary neurons

Because a previous study indicated that IL-17c provides a survival signal for colon epithelial cells in a mouse intestinal tumor model (Song et al., 2014), we tested if IL-17c has an antiapoptotic effect on neurons. During a 48-h time course of HSV-2 (strain 186) infection of mouse primary cortical neurons (MCNs), IL-17c was consistently induced throughout the time course compared with mock infected cells, with a peak induction at 6 hpi (Fig. 7 A, top). Virus titer assays suggest that HSV-2 replicated much slower in primary neurons than in primary keratinocytes (Fig. 7 A, bottom, versus Fig. 3 A, middle). Consistent with the gene expression pattern seen in laser-captured keratinocytes in skin (Fig. 2 C), IL-17a expression was not detected by quantitative RT-PCR in MCNs (not depicted). Because the receptor for IL17c is a heterodimer of IL-17RE/IL-17RA, we blocked IL-17c signaling using a

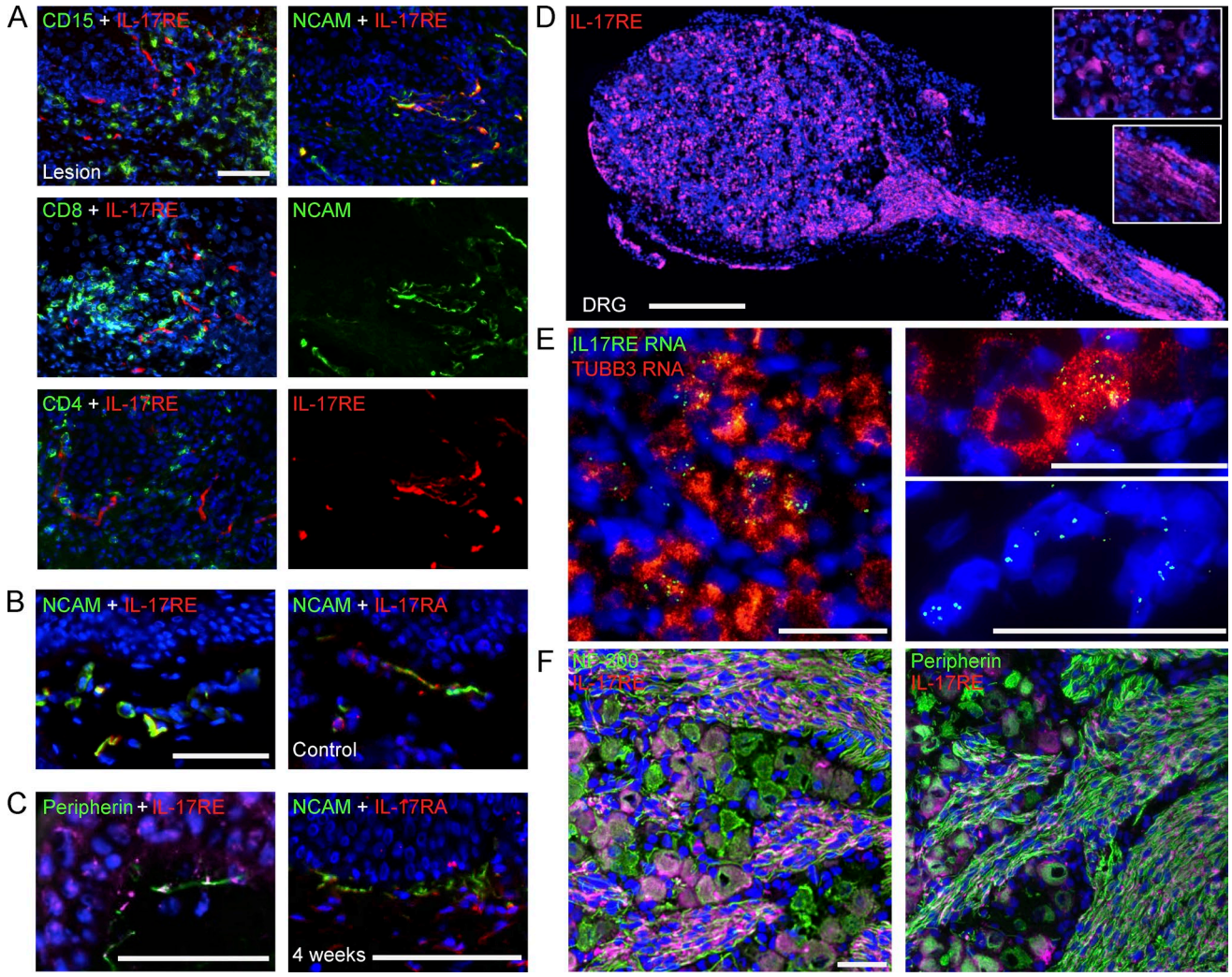

Figure 4. **Peripheral nervous systems express IL-17RE, a receptor subunit specific for IL-17c.** (A) Nerve endings in lesional genital skin expressed IL-17RE. IL-17RE$^+$ cells exhibited elongated fiber-like shapes and were distinct from CD15$^+$, CD8a$^+$, and CD4$^+$ cells. Double immunofluorescent staining with anti-IL-17RE (red) and anti-CD15, CD8a or CD4 (green) antibodies revealed no costaining (left). Double immunofluorescent staining with anti-NCAM (green) and anti-IL-17RE (red) antibodies showed significant double staining of nerve endings in lesional biopsies (right). Nuclei stained with DAPI (blue). Bar, 50 µm. (B) Nerve endings in control skin biopsies express IL-17RE and IL-17RA. Double staining with anti-NCAM and anti-IL17RE or IL-17RA antibody showed double-positive nerve endings in control skin biopsies. Bar, 50 µm. (C) Nerve endings in posthealed skin biopsies express IL-17RE and IL-17RA. Double immunofluorescent staining with anti-peripherin (green) and anti-IL-17RE (red) antibodies (left) or anti-NCAM (green) and anti-IL17RA (red) antibodies (right) revealed expression of IL-17RE on peripherin$^+$ nerve endings and expression of IL-17RA on NCAM$^+$ nerve endings in genital 4-wk posthealed skin biopsies. Nuclei stained with DAPI (blue). Bar, 50 µm. (D) Single immunofluorescent staining with anti-IL-17RE (red) in sensory neurons from human fetal DRG showed staining in both neuronal cell bodies and nerve fibers. Insets show enlarged pictures of IL-17RE expression in cell bodies (top) and axons (bottom). Bar, 500 µm. (E) Detection of IL-17RE RNA expression in sensory neurons in human fetal DRG using FISH. TUBB3, tubulin β 3 class III. Three representative images are displayed. Bars, 50 µm. (F) IL-17RE (red) expression in a subset of NF200$^+$ (left; green) or peripherin$^+$ neurons (right; green) and axons in human fetal DRG. Bar, 50 µm. All the experiments were repeated three times.

neutralizing antibody for murine IL-17RA, which had no significant effect on HSV gene expression or titers (not depicted). We then tested if pretreatment with exogenous murine IL-17c (mIL-17c) could aid in survival of neurons during HSV infection. Decreased amounts of cleaved caspase 3$^+$ cells were detected by immunofluorescence when MCNs were pretreated with mIL-17c, and the presence of a murine IL-17RA neutralizing antibody (anti-mIL17RA) eliminated this reduction (Fig. 7 B). We saw 24% reduction of neurons undergoing apoptosis with mIL-17c pretreatment before infection (Fig. 7 C, left). Pretreatment with an IL-17RA-neutralizing antibody increased neurons undergoing apoptosis by 14% during HSV-2 infection (not statistically significant; Fig. 7 C, right). HSV-2 infection in MCNs also increased enzymatic activity of caspase

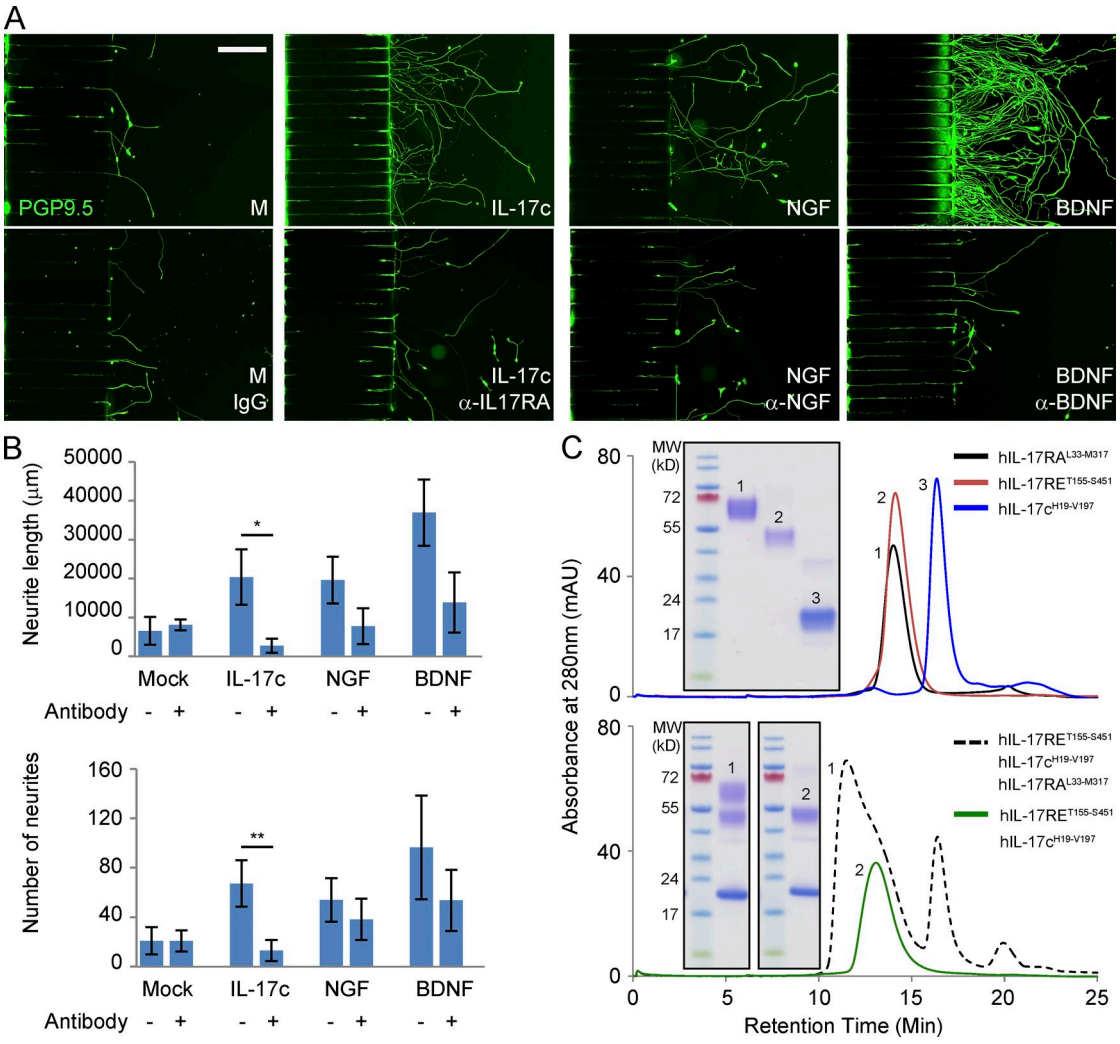

Figure 5. **IL-17c stimulated neurite growth of differentiated SY5Y neurons.** (A) IL-17c induced directional neurite growth of differentiated SY5Y cells in a microfluidic device. SY5Y cells were differentiated with all-trans retinoid acids (ATRA) at 20 µg/ml for 4 d and then placed in the wells on the left side of a microfluidic device with culture medium alone (M) or medium plus IL-17c, NGF, or BDNF with or without neutralizing antibodies for IL-17RA (α-IL17RA), NGF (α-NGF), or BDNF (α-BDNF), respectively, on the other side. After 10 d of culture, cells were fixed and stained with a PGP9.5 antibody. Bar, 200 µm. (B) Comparison of total length of neurites and numbers of neurites from all the conditions shown in A. P-value is derived from two-sample *t* test with unequal variance ($n = 3$). *, P = 0.047; **, P = 0.036. Error bars represent 1 standard deviation from the mean of three replicates. (C) Size-exclusion chromatogram (SEC) showing an overlay of the soluble forms of human IL-17c (residues 19–197), human IL-17RE (residues 155–451), and human IL-17RA (residues 33–317). Each construct runs as a well-behaved, monodispersed protein of appropriate molecular weight. Gel inset shows a fraction corresponding to each peak analyzed under nonreducing, SDS-PAGE conditions (top). SEC supershift assay showing that recombinant human IL-17c interacts both as ternary complex with IL-17RA and IL-17RE and as a binary complex with IL-17RE alone. Gel inset shows a fraction corresponding to each peak analyzed under nonreducing, SDS-PAGE conditions (bottom). All the experiments were repeated three times.

3/7, and pretreatment of murine IL-17c before infection significantly reduced this effect in an IL-17RA-dependent manner (Fig. 7 D). These findings suggest that both exogenous and endogenous murine IL-17c treatment provides a survival signal to neurons during HSV-2 infection.

DISCUSSION

Target-derived factors such as BDNF and NGF have been described to regulate neuronal cell function, including cell survival, axonal growth, and guidance, through retrograde signaling (Tessier-Lavigne and Goodman, 1996; Harrington and Ginty, 2013). Here we describe several novel observations about HSV-peripheral neuronal interactions. First, in vivo it is clear that HSV infection induces a novel functional interaction between keratinocytes and peripheral sensory neurons that involves the IL-17c/IL-17RE pathway. Our in vivo data clearly demonstrate that there is peripheral nerve growth during both clinical and subclinical HSV reactivation, pro-

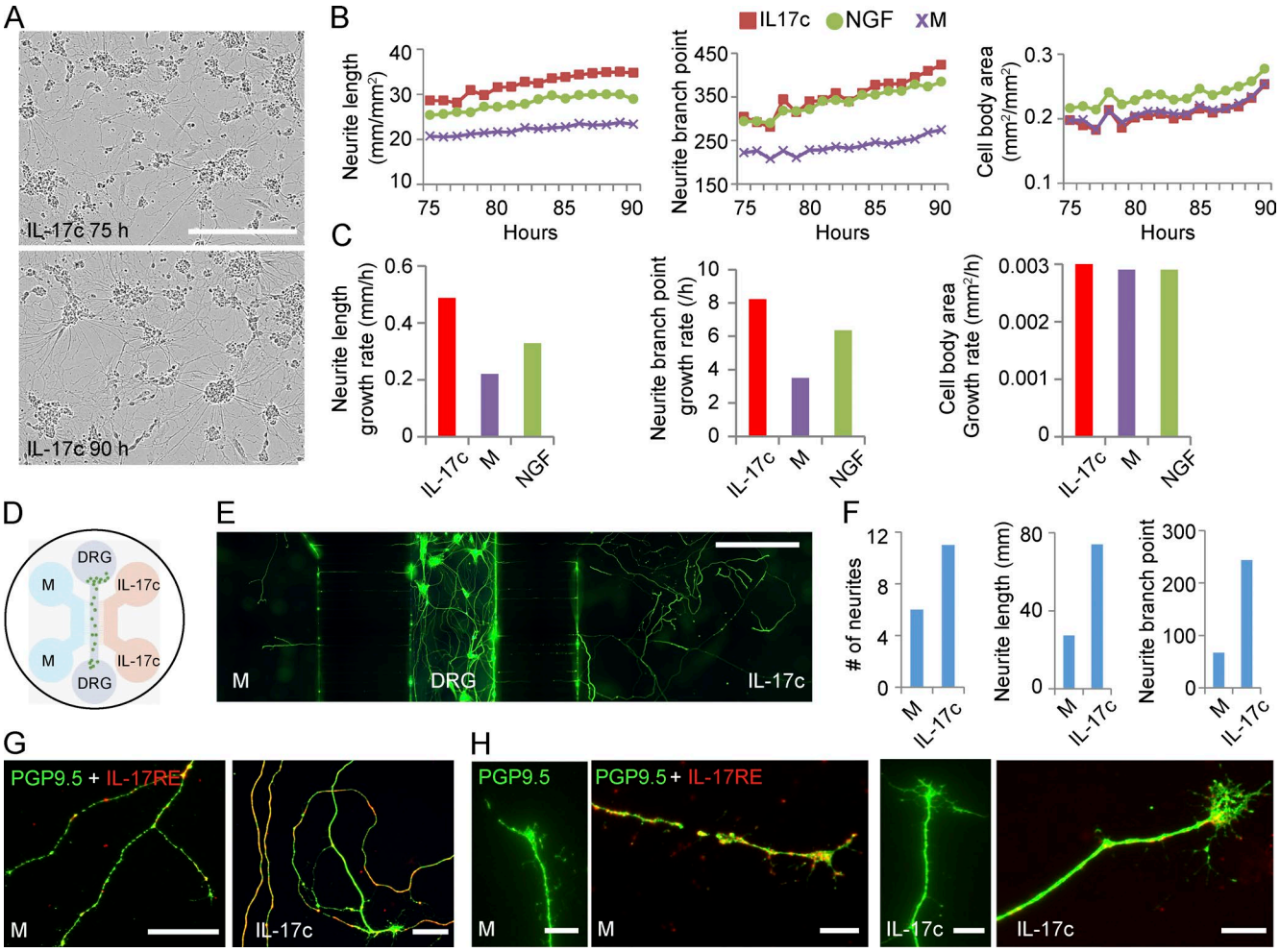

Figure 6. **IL-17c induced neurite growth and branch points in HSNs.** HSNs were isolated from fetal spinal tissue and cultured in full neural medium only or medium plus IL-17c or NGF. (A) Images of cultured HSNs in the presence of IL-17c at 75 h (top) and 90 h (bottom) after plating. Bar, 300 µm. (B) Live imaging of HSNs to measure neurite length (left graph), neurite branch points (middle graph), and cell body area (right graph) every hour for 16 h from hours 75 to 90 after HSNs were plated in culture medium or medium plus IL-17c or NGF. (C) Growth rates of neurite length (left graph), neurite branch points (middle graph), and cell body area (right graph) of cultured HSNs from hours 75 to 90 after HSNs were plated. (D) A microfluidic device with three channels. HSNs were placed in the middle channel and medium only (M) and medium plus IL-17c was placed on the left and right channels, respectively. DRG, dorsal root ganglia. (E and F) HSNs extended significantly longer neurites with more branch points into the channel with IL-17c containing medium. HSNs were fixed and stained with PGP9.5 after 16 d of culture (E) and number of neurites, total length and branch points were counted (F). Bar, 500 µm. (G and H) The HSN neurites expressed IL-17RE. HSNs in the three-channel device were double-stained with PGP9.5 and IL-17RE antibodies (G). Comparison of growth cones of neurites from medium only and IL-17c-containing channels (H). Bars, 50 µm (H), 10 µm (G). HSN experiments were repeated three times using different fetal DRG.

viding evidence that there is a process of peripheral nerve destruction and growth from HSV reactivation. Additional in vivo observations are that HSV-2 infection induces IL-17c in keratinocytes and the receptor for IL-17c is expressed on skin nerve endings located at the site of reactivation. Our ex vivo studies indicate that exogenous IL-17c induces neurite growth and that these effects on neurite growth are blocked specifically by antibodies to IL-17RA, providing plausibility that this keratinocyte–peripheral nerve interaction may be the mechanism behind our in vivo observations. One of the intriguing aspects of our data are the demonstration that nerve growth was observed over a prolonged 4–8-wk time period after healing of a lesion. The exact mechanism behind this prolonged effect remains to be determined; however, in affected areas, there is evidence for frequent if not constant release of HSV-2 into the genital tissue, potentially providing the stimulus for prolonged IL-17c production in keratinocytes locally (Schiffer et al., 2010). From a virus point of view, the stimulus of new peripheral neurites likely provides an increased exit opportunity for future reactivations (a type of viral "freedom trail"). Interestingly, HSV-2 glycoprotein G has recently been proposed to regulate growth of

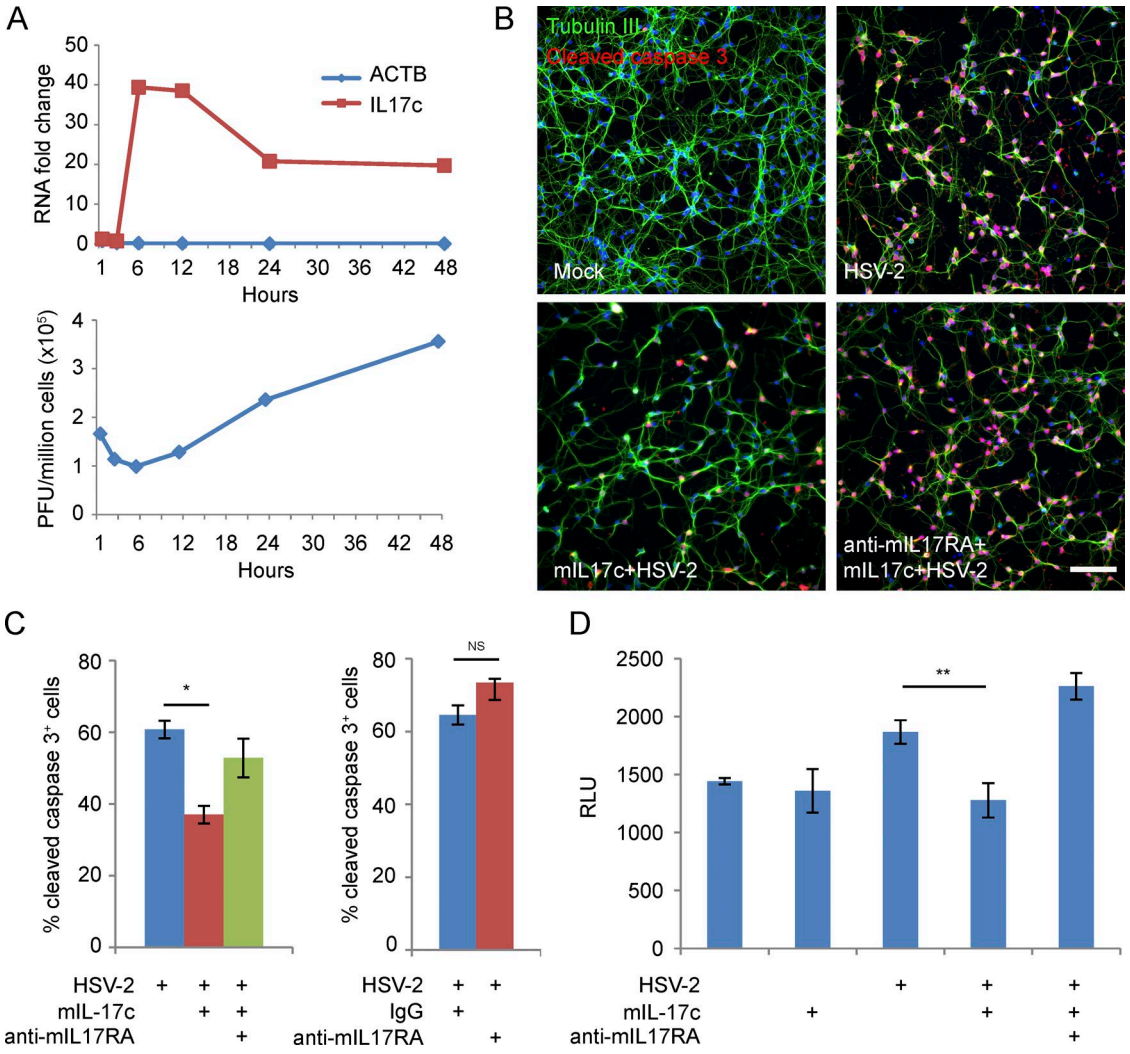

Figure 7. **IL-17c pretreatment reduces apoptosis during HSV-2 infection of MCNs.** (A) HSV-2 infection induces expression of IL-17c in MCNs. Cells were infected with HSV-2 (186) at MOI of 5 for 1, 3, 6, 12, 24, and 48 h. Y-axis is fold change over mock infected MCNs. Gene expression (IL-17c and β-actin [ACTB]) was determined by quantitative PCR (top), and virus titers were determined by plaque assays (bottom). (B) Detection by immunofluorescence of cleaved caspase 3 levels in HSV-2 (186) infected MCNs. MCNs were untreated or pretreated with mIL-17c for 24 h in the presence of a murine IL-17RA–neutralizing antibody (anti-mIL17RA) or matching control rat IgG before HSV-2 infection at MOI of 5 for 8 h. Cells were stained with DAPI for cell nucleus, an antibody for β-tubulin III to visualize neurons (green) and an antibody for cleaved caspase 3 (red). Bar, 100 µm. (C) Percentages of cleaved caspase 3^+ neurons in HSV-2 (186) infected neurons pretreated with mIL-17c (24 h) in the presence of anti-mIL17RA or control IgG (left) or pretreated with anti-IL-m17RA or control IgG (1 h; right). *, P = 0.01. (D) Detection of caspase 3/7 enzymatic activities in HSV-2 (186) infected MCNs. MCNs were treated and infected similarly as described in B and caspase 3/7 enzymatic activities were assayed by luminescence (relative light unit [RLU]). Error bars represent 1 standard deviation from the mean of three replicates. P-value is derived from two-sample *t* test with unequal variance. **, P = 0.05. The experiments were repeated three times.

free nerve endings in a mouse infection model (Cabrera et al., 2015), suggesting that IL-17c may not be the only factor involved in this regenerative process. From the host point of view, neuron survival and growth helps preserve sensory nerve function. This mutually beneficial interaction may provide a plausible mechanism for the lack of hypoesthesia associated with recurrent HSV infections and potentially explain the long-standing controversy on how HSV infection can impair peripheral nerve endings and yet not result in any clinically discernible long-standing effect on peripheral nerve function. Whether the effect of IL-17c on axonal growth can be used to improve other types of peripheral nerve dysfunctions remains to be determined. This mechanism by HSV is a natural repair and regeneration pathway for peripheral nerves that may if more completely understood have implications for treatment for and/or preventing peripheral neuropathies.

Our in vitro data suggest that HSV infection in HSN in vivo would induce the expression of IL-17c, which in turn

offers a survival signal to neurons in autocrine and paracrine manners. Skin keratinocytes also produce IL-17c during HSV infection at peripheral sites (Gaffen, 2009; Pappu et al., 2012). We show here that the antiapoptotic effect of IL-17c in neurons can be completely blocked by IL-17RA-neutralizing antibodies, suggesting that IL-17RA is required for the antiapoptotic effect of IL-17c in neurons. IL-17RE expression can be detected in nerve endings of skin biopsies during HSV-2 recurrent infection and in both cell bodies and axons in human fetal DRG. We propose that IL-17c from keratinocytes could bind to its receptors (IL-17RA/IL-17RE) on nerve endings and protect axons and cell bodies through retrograde signaling. In our in vitro studies, we demonstrated that IL-17c and IL-17RE and IL-17RA exist as a trimer, providing further plausibility that these in vitro observations are operant in vivo. We recognize that we have not presented direct proof that IL-17c from keratinocytes is the IL-17c that results in neuronal growth in vivo. However, our studies show that HSV-infected keratinocytes express the highest level of IL-17c in skin biopsy tissue. Its main receptor is expressed in vivo on neurite and/or Schwann cells, and IL-17c exhibits neurotropic activity in a wide variety of neuronal cells, including primary HSNs. Further supporting our hypothesis that IL-17c is a neurotropic factor is a recent publication demonstrating that IL-17 pathways are involved in modulating sensory neurons in *Caenorhabditis elegans* (Chen et al., 2017).

Our ex vivo data clearly indicate that IL-17c produces both peripheral nerve growth and guidance. The molecular mechanisms by which IL-17c promulgates neuronal growth are as yet unclear. Nerve regeneration/repair is a tightly coordinated molecular and cellular process that involves different cell types. The normal peripheral nerve trunk comprises complex, highly organized structures such as the endoneurium that contain axons, Schwann cells, macrophages, fibroblasts, and blood vessels. In addition, a mixture of inflammatory cells infiltrate to sites of nerve injuries, adding further complexity to this microenvironment (Zochodne, 2008; Cattin et al., 2015). Studies to dissect these interactions and their role in nerve repair are warranted. In the context of recurrent HSV-2 infection in humans, the IL-17c/IL-17RE pathway we describe appears to provide crosstalk between keratinocytes and peripheral sensory neurites that aids in nerve repair. There are significant unanswered questions regarding how IL-17c/IL-17RE pathways regulate peripheral nerve regeneration/growth in genital skin during recurrent HSV-2 infection. Although we have demonstrated the neurotrophic effects of IL-17c, it is possible that IL-17c could also be chemotactic during peripheral nerve growth. Although we show that HSV infection in keratinocytes produces IL-17c in vivo, we have not shown IL-17c induction in neurons in vivo. It is possible that IL-17c from HSV infection of ganglia cells during reactivation also plays a role in peripheral nerve growth. We have detected IL-17RE expression in both neurons and nonneuronal cells such as Schwann cells in human fetal DRG. IL-17RE also expresses in Schwann cells in addition to peripheral nerve endings in human genital skin (unpublished data). It is tempting to hypothesize that neurotrophic effects of IL-17c derive from its complex effects on multiple cell types in peripheral nerve systems. We believe that the data shown in this paper warrant further exploration on how to optimize exogenous IL-17c as a prospective neurotrophic cytokine and/or growth repair factor for peripheral nerve regeneration/repair. In summary, this work demonstrates that keratinocytes produce IL-17c, which appears to be involved in stimulating nerve growth during recurrent HSV-2 infection in humans.

MATERIALS AND METHODS

Study participants

Healthy, HSV-2 seropositive adults were recruited at the University of Washington Virology Research Clinic in Seattle. HSV-2 serostatus was determined by Western blot, as previously described (Koutsky et al., 1992); all participants were HIV seronegative, and biopsy procedures were conducted as described previously (Zhu et al., 2007; Peng et al., 2009). The biopsy protocol was approved by the University of Washington Human Subjects Review Committee, and all participants provided written consent. 3-mm punch biopsies were obtained during symptomatic recurrences from active lesion sites, newly healed lesions, and at the same sites 2, 4, 8, and 12 wk posthealing, as previously described. For biopsies taken from acute lesions, half of the biopsy included the vesicle area, and the other half covered the immediately adjacent erythematous skin area. In the posthealing time period, biopsies were obtained from the predominant lesion area, usually contiguous to the prior biopsies. Contralateral control skin biopsies were taken from normal epithelialized genital skin obtained at the same time from the opposite anatomical site from HSV reactivation. Arm control skin biopsies were taken from normal epithelialized skin from one upper arm. All samples were immediately placed on dry ice and stored at −80°C until processing.

For skin lesion biopsies, we detected HSV-2 antigen by immunofluorescence staining using rabbit antibody to HSV-2 (Dako). For posthealed asymptomatic shedding biopsies, we used a sensitive PCR assay to detect HSV-2 DNA from eight sections of each biopsy (Magaret et al., 2007).

Purification of keratinocytes from genital skin biopsies

We used a rapid immunofluorescent staining method (<15 min) to identify $CD8^+$ T cells located at the dermal epidermal junction from skin biopsies (Peng et al., 2012; Zhu et al., 2013). We then used the Zeiss PALM Microbeam LCM system to cut and catapult individual keratinocytes above the basement membrane to designated tubes in a completely automated process. Between 50 and 100 cells were captured per skin biopsy, and isolated total RNA was processed for gene expression analysis using the Illumina array platform.

RNA extraction, amplification, and hybridization of cDNA to Illumina bead arrays

Total RNA from LCM-captured keratinocytes was extracted using PicoPure RNA isolation kits according to the manu-

facturer's protocol (Applied Biosystems). The quality oftissue was analyzed by Agilent Technologies pico chips, and RNA with a quality index (RNA integrity number) greater than 5 was used. Total RNA (0.5–1 ng) was then used for cDNA synthesis using the Ovation Pico RNA Amplification System (NuGEN). The size distribution of cDNA was analyzed by Agilent Technologies nano chips, and the amplified cDNA had a Gaussian distribution with a mean size of 200 bp. The cDNA was biotin-labeled per the NuGEN protocol, and labeled cDNA (750 ng) was hybridized to Illumina HT-12 bead arrays in the Shared Resource Genome Center at the Fred Hutchison Cancer Research Center per the manufacturer's instructions.

Analysis of bead array data

Raw data were imported to GenomeStudio version 2010.3 (Illumina). Control summaries were generated to analyze the quality of hybridization. Data passing this initial quality control step were normalized using cubic spline with background subtraction. Normalized data were exported to R, and differentially expressed genes between keratinocytes from control biopsies and those from healed skin biopsies were selected using genefilter, a Bioconductor package. The differentially expressed genes were analyzed using an unsupervised hierarchical clustering method (clustering method: unweighted pair group method with arithmetic mean [weighted mean]; similarity measure: Euclidean distance) using SpotFire DecisionSite for functional genomics (version 9.1.2). Enriched functional categories and network analyses for differentially expressed genes were performed using Ingenuity Pathway Analysis (IPA 8.8). The GOMiner program was used to annotate all the 20,818 genes on Illumina Human HT-12 bead arrays. An annotation database was constructed in Microsoft Access using exported tables from GOMiner and genes that were annotated to the Gene Ontology terms "cytokine/chemokine/growth factor activity" and "cytokine/chemokine/growth factor receptor activity" were exported for further analysis in SpotFire. The array data for laser-captured keratinocytes are deposited in the National Center for Biotechnology Information's Gene Expression Omnibus (accession no. GSE98540).

Viral stocks

Viral stocks used in this study include HG52 and 186 (HSV-2); HSV-1 strains are KOS and ICP8 mutant (provided by Dr. David Knipe, Harvard Medical School, Boston, MA), ICP0 mutant (provided by Dr. William P. Halford, Southern Illinois University School of Medicine, Springfield, IL). Viral titers were determined by titration in Vero cells.

Cell cultures

Primary keratinocytes were purchased from Lifeline Cell Technology. Cells were cultured in DermaLife Basal Medium with DermaLife K LifeFactors (catalog no. LS-1030), as recommended by the manufacturer. Acyclovir stock solution was prepared in DMSO at 6.76 mg/ml (30 mM; Sigma-Aldrich) and diluted 1:1,000 for use on primary keratinocytes (30 μM). To UV-treat a virus stock, HG52 virus stock was spread on a tissue culture–grade 60-mm Petri dish. With the Petri dish lid off, a UV light source was placed 2 inches above the virus for 30 min. UV-treated virus was stored at −80°C for later use.

Primary MCNs were purchased from Thermo Fisher Scientific and cultured as recommended by the manufacturer. To block IL-17c signaling, cells were treated with a neutralizing antibody for IL-17RA (rat monoclonal antibody) and matching rat control IgG (R&D Systems; 2 μg/ml) for 1 h before HSV infection. mIL-17c was expressed and purified at the Molecular Design and Therapeutics facility at the Fred Hutchinson Cancer Research Center (Fig. S1). To detect apoptosis during HSV-2 (186) infection of mouse primary neurons, cells were stained with an antibody for cleaved caspase 3 (Cell Signaling Technology) according to the manufacturer's methods.

TLR ligands were purchased from InvivoGen (PGN, catalog no. tlrl-pgnsa; poly[I:C], catalog no. tlrl-pic; poly[I:C]/LyoVec, Catalog no. tlrl-piclv; LPS, catalog no. tlrl-pb5lps; flagellin, catalog no. tlrl-epstfla; ODN, catalog no. tlrl-2395). For TLR stimulation, cells were treated with PGN (2 μg/ml), poly(I:C)/LyoVec (250 ng/ml), poly(I:C) (200 ng/ml), LPS (100 ng/ml), flagellin (50 ng/ml), and ODN (1 μM) for 2, 6, and 24 h. For combination of HSV-2 (HG-52) and TLR stimulation, cells were infected with HG-52 (MOI of 2) for 3 h, and TLR ligands (poly[I:C]/LyoVec, poly[I:C], and flagellin) were added for 4 h before cells were lysed for total RNA extraction.

Human SH-SY5Y neuroblastoma cells were obtained from ATCC. The SH-SY5Y neuroblastoma cell lines were maintained in 1:1 mixture of ATCC-formulated EMEM and F12 media containing 15% (vol/vol) heat-inactivated FBS without antibiotics. SH-SY5Y cells were induced to differentiate up to 7 d with 50 μm all-*trans* retinoic acid (Sigma-Aldrich) in 1:1 mixture EMEM/F12 media supplemented with 5% (vol/vol) FBS without antibiotics. They were monitored daily by phase-contrast microscopy for the appearance of elongated neurites. A differentiated cell was defined as a cell with a neurite length greater than the length of the cell body (on average greater than 10 μm in length) and expressing β-tubulin III (Abcam).

Isolation of human fetal DRG and sensory neurons

Human fetal spinal cords were isolated from first- and early second-trimester aborted specimens, obtained from the Laboratory of Developmental Biology in full compliance with the ethical guidelines of the National Institutes of Health and with the approval of the University of Washington institutional review boards for the collection and distribution of human tissues for research. The Laboratory of Developmental Biology obtained written consent from all tissue donors. The tissue was briefly washed in HBSS and transported in Hibernate E at 4°C before isolation of DRG.

All ganglia were dissected under sterile conditions, dissected free of fascia and connective tissue, and collected in DMEM and digested in 0.25% trypsin solution for 30 min at 37°C, washed in culture medium containing 10% FBS, and then triturated into a single-cell suspension with a fire-polished glass Pasteur pipet. Cells were resuspended in Neurobasal media (Thermo Fisher Scientific) supplemented with B27 and 0.5 mM Glutamax (with antibiotics) and counted with trypan blue assay. Cell suspensions were plated in poly-D-lysine- and laminin-coated eight-well chamber slides (BD/Corning) in Neurobasal/B27 media supplemented with 50 ng/ml human β-NGF (EMD Millipore) and incubated overnight at 37°C. For each experiment, the cells were washed twice with basal media before addition of PBS or recombinant human IL-17c (200 ng/ml [eBioscience] or synthesized at the Fred Hutchinson Cancer Research Center Shared Resource facility). Identification of the cells as neurons was confirmed by showing reactivity on the neurites with monoclonal antibody for PGP9.5.

Culture of neurons in microfluidic chambers

Microfluidic chambers (Xona Microfluidic) were autoclaved and bonded into FluoroDish (World Precision Instruments) using a laboratory Corona treater (Electro-Technic Products). Microfluidic chambers were coated with 1% (vol/vol) polyethylenimine for 10 min and 0.1% (vol/vol) glutaraldehyde for 30 min to provide adhesion to the collagen gels. Rat tail collagen I (Gibco) was perfused through microfluidic chambers at a concentration of 5 μg/cm^2. Twenty microliters of 2,000,000 cells/ml differentiated SY5Y cells were seeded into the soma channel. After 10 min, 50 μl culture media was added into each soma reservoir, and 70 μl culture media with 200 ng/ml IL-17c (eBioscience or synthesized at the Fred Hutchinson Cancer Research Center) or NGF (10 ng/ml) or BDNF (20 ng/ml; both from PeproTech) or the same volume of PBS was added into each distal reservoir with control IgG or neutralizing antibodies for IL-17RA (2 μg/ml), NGF, or BDNF (1 μg/ml), respectively (anti-human IL-17RA from R&D Systems; anti-NGF and anti-BDNF from PeproTech). Half of the growth media was changed every other day. 10 d later, cultures were fixed and stained with a PGP9.5 antibody.

For human primary fetal neuron culture, three-channel microfluidic chambers (Xona Microfluidic) were autoclaved and bonded onto clean coverslips (Corning) using a plasma cleaner (Harrick Scientific). The chambers were sterilized with 70% ethanol and then coated with 0.5 mg/ml poly-D-lysine (Corning) and 10 μg/ml mouse laminin (Thermo Fisher Scientific). Dissociated human fetal DRG neurons were plated into the middle channel at a density of 100,000 cells/chamber. After 4 d, 200 ng/ml IL-17c was added into the right channel to generate a gradient of IL-17c in the soma (middle) channel. Half of the growth media was changed every other day. Sixteen days later, cultures were fixed and stained.

Time-lapse microscopy

Long-term kinetic imaging of cultivated human neurons grown in eight-well chamber slides inside a conventional tissue culture incubator was performed with an Incucyte microscope system (Essen Bioscience) fitted with a Nikon 10×/0.3 Plan Fluor objective. Bright-field images were collected at 1-h intervals. Four fields of view were imaged in phase contrast for each well, and mean neurite length and number of branch points were measured with the Incucyte neuro-track image analysis software module.

Slide scanning and cytometric analysis

To quantify IL-17c$^+$ or cleaved caspase 3$^+$ cells, 30,000 keratinocytes or 80,000 MCNs were cultured overnight or for 3 d in 8-well chamber slides before IL-17c pretreatment and/or HSV-2 (strain HG52 or 186) infection (MOIs of 2 and 5 for keratinocytes and MCNs, respectively). MCNs were pretreated with mIL-17c at 20 ng/ml in the presence of murine IL-17RA–neutralizing antibody (2 μg/ml) or matching control rat IgG (2 μg/ml) for 24 h before infection. Slides were scanned on a TissueFAXS microscope system (TissueGnostics) consisting of a Zeiss Imager Z2 upright fluorescence microscope, motorized Marzhauser stage with eight-slide capacity, and PCO pixelfly QE charge-coupled device camera. System operation was controlled by TissueFAXS software, which provided automated large area acquisition with image stitching and autofocus. Images were acquired with a Zeiss Plan Apochromat 10×/0.45 objective. Zeiss fluorescence filter sets for DAPI, FITC (for GFP), and Cy5 (for IL-17c and cleaved caspase 3) were used.

Image analysis was performed with TissueGnostics TissueQuest software. Whole-slide scans were imported into TissueQuest. Images were segmented, and cells were identified by setting appropriate intensity thresholds and cell size parameters for all channels. Live cells were identified and counted on the basis of nuclear channel staining (DAPI). Mean staining intensity of the green and far red channels was measured for all segmented objects (cells). Typically, a cell mask including nucleus and cytoplasm was used. In some cases in which the staining was predominantly cytoplasmic and cell size and shape was very heterogeneous, a ring mask derived from the nuclear mask was used to sample mean staining intensity in the cytoplasm. Once all cell data had been obtained, intensity values for the desired channels were plotted for all cells as density plot using the sm package in R, and appropriate cutoffs were set to obtain counts and percentages of positive cells. DAPI$^+$ cells were counted as live neurons and cleaved caspase 3$^+$ cells were counted as neurons under apoptosis. The accuracy of the algorithms was verified by performing manual counts of selected regions and comparing them with the output of the TissueQuest software; there was good agreement between the two methods.

Immunofluorescent staining

The staining methods were previously described (Zhu et al., 2007, 2009, 2013; Peng et al., 2012). The antibodies for

staining were purchased from the following sources: IL-17c antibody (mouse monoclonal, R&D Systems); IL-17RE antibody (rabbit polyclonal, Sigma-Aldrich); IL-17RA antibody (rabbit monoclonal, LifeSpanBioSciences); NCAM antibody (mouse monoclonal, BD); PGP9.5 (Abcam); NF200 antibody (rabbit polyclonal, Sigma-Aldrich); Peripherin antibody (rabbit and mouse, Sigma-Aldrich); cleaved caspase 3 antibody (rabbit polyclonal, Cell Signaling Technology).

Quantitative RT-PCR assay

Total RNA was extracted from human primary keratinocytes and mouse cortical neurons using QIAGEN RNeasy mini kits. cDNA was synthesized from total RNA using high-capacity cDNA synthesis kits (Applied Biosystems). The TaqMan probes for *ACTB*, *IL-17c*, and *IL-17RE* were ordered from Applied Biosystems (inventoried primer-probes). The gene expression was normalized to ACTB.

Semiautomated measurements of nerve fiber density in skin biopsy

Tissue sections chosen from each biopsy were immunoassayed with polyclonal anti–neural cell adhesion molecule (NCAM; BD) antibody (1:100 dilution), using the Tyramide Signal Amplification (Invitrogen) method for fluorescence immunohistochemistry. Sections were analyzed and captured on Leica DMR at 20× magnification. Nerve fiber density (defined as millimeters/millimeter per section) across the entire dermal-epidermal junction was calculated by using the application Simple Neurite Tracer on 2D images. This plugin is free software, licensed under the GNU General Public License version 3 and based on the public domain image processing software Fiji ImageJ. The software and step-by-step instructions are available at http://fiji.sc/Simple_Neurite_Tracer and http://pacific.mpi-cbg.de. In brief, to trace a nerve fiber (neuronal path), both the starting and end points or successive points along the midline of a neural process were selected and pixels generated converted to micrometers.

Fluorescence in situ hybridization (FISH)

Fresh frozen skin biopsies or fetal DRG were cyrosectioned into 10-µm slides, fixed with chilled 10% buffered formalin (Thermo Fisher Scientific), dehydrate in ethanol series, pretreated with protease K, and hybridized using RNAscope multiplex fluorescent assay (Advanced Cell Diagnostics), according to the manufacturer's instruction. The probes used were human IL-17RE, human TUBB3-C2, positive control PPIB, and negative control DapB (all from Advanced Cell Diagnostics).

Enzymatic assay to detect apoptosis

The caspase 3/7 assay kit was purchased from Promega (catalog no. G8091). MCNs (20,000 cells per well in 96-well plates) were pretreated with mIL-17c for 24 h and then infected with HSV-2 (strain 186) at an MOI of 5 for 8 h. The biochemical reactions were performed according to the manufacturer's instructions. The luminescent signals were detected using a BioTek synergy HT4 machine (BioTek Instruments) according to the manufacturer's instructions.

Protein expression and binding assays

Human IL-17c (residues His19–Val197), mIL-17c (residues His15–Val194), and human IL-17RA (residues Leu33–Met317) were gene synthesized with C-terminal TEV-HIS-AVI tags and expressed as soluble proteins using the Daedalus expression system and purified using HisTrap FF crude affinity columns (Bandaranayake et al., 2011). Human IL-17RE (Thr155–Ser451) was successfully secreted as a C-terminal fusion protein with human Siderocalin (Fig. S1). Purified fusion protein was then cleaved with TEV protease and separated by size-exclusion chromatography. All size-exclusion chromatography experiments were run on an AKTA Pure M equipped with a Superdex 200 Increase 10/300 GL column. SDS-PAGE analysis was done using NuPAGE 4%–12% Bis-Tris gels run under nonreducing conditions according to the manufacturer's protocols.

Online supplemental material

Fig. S1 is a schematic showing IL-17c and its receptors (IL-17RA and IL-17RE) expression constructs used in the study. Table S1 lists the patient characteristics in the study.

ACKNOWLEDGMENTS

We thank M. Miner for editing and J. Olson and A. Bandaranayake for helpful conversations. We also thank our study participants.

This work was supported by grants from the National Institutes of Health (R01 AI042528, R01 AI111780, and PO1 AI030731) and the James B. Pendleton Charitable Trust. The Laboratory of Developmental Biology was supported by National Institutes of Health award 5R24HD000836 from the Eunice Kennedy Shriver National Institute of Child Health and Human Development. D.M. Knipe was supported by National Institutes of Health grant AI063106.

The authors declare no competing financial interests.

Submitted: 22 April 2016

Revised: 22 March 2017

Accepted: 24 May 2017

REFERENCES

Abemayor, E., and N. Sidell. 1989. Human neuroblastoma cell lines as models for the in vitro study of neoplastic and neuronal cell differentiation. *Environ. Health Perspect.* 80:3–15. http://dx.doi.org/10.1289/ehp.89803

Bandaranayake, A.D., C. Correnti, B.Y. Ryu, M. Brault, R.K. Strong, and D.J. Rawlings. 2011. Daedalus: a robust, turnkey platform for rapid production of decigram quantities of active recombinant proteins in human cell lines using novel lentiviral vectors. *Nucleic Acids Res.* 39:e143. http://dx.doi.org/10.1093/nar/gkr706

Cabrera, J.R., A. Viejo-Borbolla, N. Martinez-Martín, S. Blanco, F. Wandosell, and A. Alcamí. 2015. Secreted herpes simplex virus-2 glycoprotein G modifies NGF-TrkA signaling to attract free nerve endings to the site of infection. *PLoS Pathog.* 11:e1004571. http://dx.doi.org/10.1371/journal.ppat.1004571

Cattin, A.L., J.J. Burden, L. Van Emmenis, F.E. Mackenzie, J.J. Hoving, N. Garcia Calavia, Y. Guo, M. McLaughlin, L.H. Rosenberg, V. Quereda,

et al. 2015. Macrophage-induced blood vessels guide Schwann cell-mediated regeneration of peripheral nerves. *Cell.* 162:1127–1139. http://dx.doi.org/10.1016/j.cell.2015.07.021

Chang, S.H., J.M. Reynolds, B.P. Pappu, G. Chen, G.J. Martinez, and C. Dong. 2011. Interleukin-17C promotes Th17 cell responses and autoimmune disease via interleukin-17 receptor E. *Immunity.* 35:611–621. http://dx.doi.org/10.1016/j.immuni.2011.09.010

Chen, C., E. Itakura, G.M. Nelson, M. Sheng, P. Laurent, L.A. Fenk, R.A. Butcher, R.S. Hegde, and M. de Bono. 2017. IL-17 is a neuromodulator of *Caenorhabditis elegans* sensory responses. *Nature.* 542:43–48. http://dx.doi.org/10.1038/nature20818

Chuong, C.M., B.J. Nickoloff, P.M. Elias, L.A. Goldsmith, E. Macher, P.A. Maderson, J.P. Sundberg, H. Tagami, P.M. Plonka, K. Thestrup-Pederson, et al. 2002. What is the 'true' function of skin? *Exp. Dermatol.* 11:159–187.

Gaffen, S.L. 2009. Structure and signalling in the IL-17 receptor family. *Nat. Rev. Immunol.* 9:556–567. http://dx.doi.org/10.1038/nri2586

Gaffen, S.L. 2011. Recent advances in the IL-17 cytokine family. *Curr. Opin. Immunol.* 23:613–619. http://dx.doi.org/10.1016/j.coi.2011.07.006

Haanpää, M., P. Laippala, and T. Nurmikko. 1999. Pain and somatosensory dysfunction in acute herpes zoster. *Clin. J. Pain.* 15:78–84. http://dx.doi.org/10.1097/00002508-199906000-00003

Harrington, A.W., and D.D. Ginty. 2013. Long-distance retrograde neurotrophic factor signalling in neurons. *Nat. Rev. Neurosci.* 14:177–187. http://dx.doi.org/10.1038/nrn3253

Johnston, A., Y. Fritz, S.M. Dawes, D. Diaconu, P.M. Al-Attar, A.M. Guzman, C.S. Chen, W. Fu, J.E. Gudjonsson, T.S. McCormick, and N.L. Ward. 2013. Keratinocyte overexpression of IL-17C promotes psoriasiform skin inflammation. *J. Immunol.* 190:2252–2262. http://dx.doi.org/10.4049/jimmunol.1201505

Johnston, C., M. Saracino, S. Kuntz, A. Magaret, S. Selke, M.L. Huang, J.T. Schiffer, D.M. Koelle, L. Corey, and A. Wald. 2012. Standard-dose and high-dose daily antiviral therapy for short episodes of genital HSV-2 reactivation: three randomised, open-label, cross-over trials. *Lancet.* 379:641–647. http://dx.doi.org/10.1016/S0140-6736(11)61750-9

Koutsky, L.A., C.E. Stevens, K.K. Holmes, R.L. Ashley, N.B. Kiviat, C.W. Critchlow, and L. Corey. 1992. Underdiagnosis of genital herpes by current clinical and viral-isolation procedures. *N. Engl. J. Med.* 326:1533–1539. http://dx.doi.org/10.1056/NEJM199206043262305

Kurt-Jones, E.A., M. Chan, S. Zhou, J. Wang, G. Reed, R. Bronson, M.M. Arnold, D.M. Knipe, and R.W. Finberg. 2004. Herpes simplex virus 1 interaction with Toll-like receptor 2 contributes to lethal encephalitis. *Proc. Natl. Acad. Sci. USA.* 101:1315–1320. http://dx.doi.org/10.1073/pnas.0308057100

Lloyd, C., Q.C. Yu, J. Cheng, K. Turksen, L. Degenstein, E. Hutton, and E. Fuchs. 1995. The basal keratin network of stratified squamous epithelia: defining K15 function in the absence of K14. *J. Cell Biol.* 129:1329–1344. http://dx.doi.org/10.1083/jcb.129.5.1329

Lund, J., A. Sato, S. Akira, R. Medzhitov, and A. Iwasaki. 2003. Toll-like receptor 9-mediated recognition of Herpes simplex virus-2 by plasmacytoid dendritic cells. *J. Exp. Med.* 198:513–520. http://dx.doi.org/10.1084/jem.20030162

Magaret, A.S., A. Wald, M.L. Huang, S. Selke, and L. Corey. 2007. Optimizing PCR positivity criterion for detection of herpes simplex virus DNA on skin and mucosa. *J. Clin. Microbiol.* 45:1618–1620. http://dx.doi.org/10.1128/JCM.01405-06

Misery, L. 1997. Skin, immunity and the nervous system. *Br. J. Dermatol.* 137:843–850. http://dx.doi.org/10.1111/j.1365-2133.1997.tb01542.x

Pappu, R., S. Rutz, and W. Ouyang. 2012. Regulation of epithelial immunity by IL-17 family cytokines. *Trends Immunol.* 33:343–349. http://dx.doi.org/10.1016/j.it.2012.02.008

Peng, T., J. Zhu, A. Klock, K. Phasouk, M.L. Huang, D.M. Koelle, A. Wald, and L. Corey. 2009. Evasion of the mucosal innate immune system by herpes simplex virus type 2. *J. Virol.* 83:12559–12568. http://dx.doi.org/10.1128/JVI.00939-09

Peng, T., J. Zhu, K. Phasouk, D.M. Koelle, A. Wald, and L. Corey. 2012. An effector phenotype of CD8+ T cells at the junction epithelium during clinical quiescence of herpes simplex virus 2 infection. *J. Virol.* 86:10587–10596. http://dx.doi.org/10.1128/JVI.01237-12

Ramirez-Carrozzi, V., A. Sambandam, E. Luis, Z. Lin, S. Jeet, J. Lesch, J. Hackney, J. Kim, M. Zhou, J. Lai, et al. 2011. IL-17C regulates the innate immune function of epithelial cells in an autocrine manner. *Nat. Immunol.* 12:1159–1166. http://dx.doi.org/10.1038/ni.2156

Rasmussen, S.B., S.B. Jensen, C. Nielsen, E. Quartin, H. Kato, Z.J. Chen, R.H. Silverman, S. Akira, and S.R. Paludan. 2009. Herpes simplex virus infection is sensed by both Toll-like receptors and retinoic acid-inducible gene-like receptors, which synergize to induce type I interferon production. *J. Gen. Virol.* 90:74–78. http://dx.doi.org/10.1099/vir.0.005389-0

Reinert, L.S., L. Harder, C.K. Holm, M.B. Iversen, K.A. Horan, F. Dagnæs-Hansen, B.P. Ulhøi, T.H. Holm, T.H. Mogensen, T. Owens, et al. 2012. TLR3 deficiency renders astrocytes permissive to herpes simplex virus infection and facilitates establishment of CNS infection in mice. *J. Clin. Invest.* 122:1368–1376. http://dx.doi.org/10.1172/JCI60893

Roizman, B., and R.J. Whitley. 2013. An inquiry into the molecular basis of HSV latency and reactivation. *Annu. Rev. Microbiol.* 67:355–374. http://dx.doi.org/10.1146/annurev-micro-092412-155654

Sato, A., M.M. Linehan, and A. Iwasaki. 2006. Dual recognition of herpes simplex viruses by TLR2 and TLR9 in dendritic cells. *Proc. Natl. Acad. Sci. USA.* 103:17343–17348. http://dx.doi.org/10.1073/pnas.0605102103

Schiffer, J.T., L. Abu-Raddad, K.E. Mark, J. Zhu, S. Selke, D.M. Koelle, A. Wald, and L. Corey. 2010. Mucosal host immune response predicts the severity and duration of herpes simplex virus-2 genital tract shedding episodes. *Proc. Natl. Acad. Sci. USA.* 107:18973–18978. http://dx.doi.org/10.1073/pnas.1006614107

Schiffer, J.T., D. Swan, R. Al Sallaq, A. Magaret, C. Johnston, K.E. Mark, S. Selke, N. Ocbamichael, S. Kuntz, J. Zhu, et al. 2013. Rapid localized spread and immunologic containment define Herpes simplex virus-2 reactivation in the human genital tract. *eLife.* 2:e00288. http://dx.doi.org/10.7554/eLife.00288

Schmader, K. 1998. Postherpetic neuralgia in immunocompetent elderly people. *Vaccine.* 16:1768–1770. http://dx.doi.org/10.1016/S0264-410X(98)00137-6

Song, X., S. Zhu, P. Shi, Y. Liu, Y. Shi, S.D. Levin, and Y. Qian. 2011. IL-17RE is the functional receptor for IL-17C and mediates mucosal immunity to infection with intestinal pathogens. *Nat. Immunol.* 12:1151–1158. http://dx.doi.org/10.1038/ni.2155

Song, X., H. Gao, Y. Lin, Y. Yao, S. Zhu, J. Wang, Y. Liu, X. Yao, G. Meng, N. Shen, et al. 2014. Alterations in the microbiota drive interleukin-17C production from intestinal epithelial cells to promote tumorigenesis. *Immunity.* 40:140–152. http://dx.doi.org/10.1016/j.immuni.2013.11.018

Svensson, A., P. Tunbäck, I. Nordström, L. Padyukov, and K. Eriksson. 2012. Polymorphisms in Toll-like receptor 3 confer natural resistance to human herpes simplex virus type 2 infection. *J. Gen. Virol.* 93:1717–1724. http://dx.doi.org/10.1099/vir.0.042572-0

Tessier-Lavigne, M., and C.S. Goodman. 1996. The molecular biology of axon guidance. *Science.* 274:1123–1133. http://dx.doi.org/10.1126/science.274.5290.1123

Wald, A., L. Corey, R. Cone, A. Hobson, G. Davis, and J. Zeh. 1997. Frequent genital herpes simplex virus 2 shedding in immunocompetent women. Effect of acyclovir treatment. *J. Clin. Invest.* 99:1092–1097. http://dx.doi.org/10.1172/JCI119237

Zhu, J., D.M. Koelle, J. Cao, J. Vazquez, M.L. Huang, F. Hladik, A. Wald, and L. Corey. 2007. Virus-specific CD8+ T cells accumulate near sensory

nerve endings in genital skin during subclinical HSV-2 reactivation. *J. Exp. Med.* 204:595–603. http://dx.doi.org/10.1084/jem.20061792

Zhu, J., F. Hladik, A. Woodward, A. Klock, T. Peng, C. Johnston, M. Remington, A. Magaret, D.M. Koelle, A. Wald, and L. Corey. 2009. Persistence of HIV-1 receptor-positive cells after HSV-2 reactivation is a potential mechanism for increased HIV-1 acquisition. *Nat. Med.* 15:886–892. http://dx.doi.org/10.1038/nm.2006

Zhu, J., T. Peng, C. Johnston, K. Phasouk, A.S. Kask, A. Klock, L. Jin, K. Diem, D.M. Koelle, A. Wald, et al. 2013. Immune surveillance by CD8αα+ skin-resident T cells in human herpes virus infection. *Nature.* 497:494–497. http://dx.doi.org/10.1038/nature12110

Zochodne, D.W. 2008. Neurobiology of Peripheral Nerve Regeneration. Cambridge University Press, Cambridge, UK. http://dx.doi.org/10.1017/CBO9780511541759